

Avoiding Kernel Fixed Points: Computing with ELU and GELU Infinite Networks

Russell Tsuchida¹, Tim Pearce², Christopher Van Der Heide³, Fred Roosta^{3, 4}, and Marcus Gallagher¹

¹School of Information Technology and Electrical Engineering, The University of Queensland

²Department of Engineering, University of Cambridge

³School of Mathematics and Physics, The University of Queensland

⁴International Computer Science Institute, University of California, Berkeley

Abstract

Analysing and computing with Gaussian processes arising from infinitely wide neural networks has recently seen a resurgence in popularity. Despite this, many explicit covariance functions of networks with activation functions used in modern networks remain unknown. Furthermore, while the kernels of deep networks can be computed iteratively, theoretical understanding of deep kernels is lacking, particularly with respect to fixed-point dynamics. Firstly, we derive the covariance functions of MLPs with exponential linear units and Gaussian error linear units and evaluate the performance of the limiting Gaussian processes on some benchmarks. Secondly, and more generally, we introduce a framework for analysing the fixed-point dynamics of iterated kernels corresponding to a broad range of activation functions. We find that unlike some previously studied neural network kernels, these new kernels exhibit non-trivial fixed-point dynamics which are mirrored in finite-width neural networks.¹

1 Introduction

We begin by reviewing the connection between infinitely wide neural networks and Gaussian processes (GPs). Once the basic setting, its extensions, and some outstanding problems have been described, we discuss our contributions.

¹Software available at https://github.com/RussellTsuchida/ELU_GELU_kernels.

1.1 Background

1.1.1 Basic setting

Consider a one-hidden layer network. Suppose each i th row of weights \mathbf{W}_i together with the corresponding bias B_i in the hidden layer has distribution $(\mathbf{W}_i^\top, B_i)^\top = \widetilde{\mathbf{W}}_i \sim \mathcal{N}(\mu, \Sigma)$, with $\Sigma \succ 0$ being a diagonal matrix having a unique “square root” $\Sigma^{(1/2)}$. Further, suppose each weight/bias vector is independent from one another. Finally, suppose the output layer parameter vector $\mathbf{V} = \frac{1}{\sqrt{n}} \mathbf{U}$ satisfies $\mathbf{U} \sim \mathcal{N}(\mathbf{0}, \sigma_w^2 I)$, where n is the number of neurons in the hidden layer and the output bias satisfies $V_b \sim \mathcal{N}(0, \sigma_b^2)$.

The output evaluated at input \mathbf{x}_1 is

$$f(\mathbf{x}_1) = \frac{1}{\sqrt{n}} \sum_{i=1}^n U_i \psi(\widetilde{\mathbf{W}}_i^\top \widetilde{\mathbf{x}}_1) + V_b,$$

where ψ is some activation function and $\widetilde{\mathbf{x}}_1 = (\mathbf{x}_1^\top, 1)^\top$. The covariance between any two outputs is given by

$$\begin{aligned} k^{(1)}(\mathbf{x}_1, \mathbf{x}_2) &= \mathbb{E} \left[\sum_{i=1}^n V_i \psi(\widetilde{\mathbf{W}}_i^\top \widetilde{\mathbf{x}}_1) \sum_{j=1}^n V_j \psi(\widetilde{\mathbf{W}}_j^\top \widetilde{\mathbf{x}}_2) \right] + \sigma_b^2 \\ &= \mathbb{E} \left[\frac{\sigma_w^2}{n} \sum_{i=1}^n \psi(\widetilde{\mathbf{W}}_i^\top \widetilde{\mathbf{x}}_1) \psi(\widetilde{\mathbf{W}}_i^\top \mathbf{x}_2) \right] + \sigma_b^2 \\ &= \sigma_w^2 \mathbb{E} \left[\psi(\widetilde{\mathbf{W}}_1^\top \widetilde{\mathbf{x}}_1) \psi(\widetilde{\mathbf{W}}_1^\top \widetilde{\mathbf{x}}_2) \right] + \sigma_b^2. \end{aligned}$$

Letting \mathbf{G} denote a $(d+1)$ –element standard Gaussian random vector with independent entries, $k^{(1)}(\mathbf{x}_1, \mathbf{x}_2)$ is

$$\sigma_w^2 \mathbb{E} \left[\psi(\mathbf{G}^\top \Sigma^{(1/2)} \widetilde{\mathbf{x}}_1 + \boldsymbol{\mu}^\top \widetilde{\mathbf{x}}_1) \psi(\mathbf{G}^\top \Sigma^{(1/2)} \widetilde{\mathbf{x}}_2 + \boldsymbol{\mu}^\top \widetilde{\mathbf{x}}_2) \right] + \sigma_b^2.$$

The expectation over $d+1$ random variables reduces to an expectation over 2 random variables, $\mathbf{G}^\top \Sigma^{(1/2)} \widetilde{\mathbf{x}}_1$ and $\mathbf{G}^\top \Sigma^{(1/2)} \widetilde{\mathbf{x}}_2$. The joint distribution of these two

random variables is a bivariate Gaussian. The mean of each component is zero, and the variance is $\|\Sigma^{(1/2)}\tilde{\mathbf{x}}_i\|^2$, where $\|\cdot\|$ denotes the Euclidean norm. The covariance is $\|\Sigma^{(1/2)}\tilde{\mathbf{x}}_1\|\|\Sigma^{(1/2)}\tilde{\mathbf{x}}_2\|\cos\theta$, where θ is the angle between $\Sigma^{(1/2)}\tilde{\mathbf{x}}_1$ and $\Sigma^{(1/2)}\tilde{\mathbf{x}}_2$. Therefore, the expectation in terms of $\mathbf{Z} \sim \mathcal{N}(\mathbf{0}, S)$ is

$$k^{(1)}(\mathbf{x}_1, \mathbf{x}_2) = \sigma_w^2 \mathbb{E} \left[\psi(s_1 Z_1 + \tilde{\mu}_1) \psi(s_2 Z_2 + \tilde{\mu}_2) \right] + \sigma_b^2, \quad (1)$$

where S has diagonals 1 and off-diagonals $\cos\theta$, and $s_i = \|\Sigma^{(1/2)}\tilde{\mathbf{x}}_i\|$ and $\tilde{\mu}_i = \boldsymbol{\mu}^\top \tilde{\mathbf{x}}_i$.

Definition 1. We call (1) the kernel and $\cos\theta^{(1)} = \frac{k^{(1)}(\mathbf{x}_1, \mathbf{x}_2)}{\sqrt{k^{(1)}(\mathbf{x}_1, \mathbf{x}_1)k^{(1)}(\mathbf{x}_2, \mathbf{x}_2)}}$ the normalised kernel.

Briefly reproducing a celebrated argument (Neal, 1995), the neural network converges to a GP as $n \rightarrow \infty$ under mild conditions on the input and activation function. Since $f(\mathbf{x}_1)$ is a sum of independent random variables scaling as $n^{-1/2}$, it converges to a Gaussian random variable with zero mean as $n \rightarrow \infty$. More generally, any collection of N evaluations of f , $\{f(\mathbf{x}_i)\}_{i=1}^N$ converges to an N -variate $\mathbf{0}$ -mean Gaussian as $n \rightarrow \infty$.

Analytical and closed-form covariance functions (1) are available for specific choices of ψ (Le Roux and Bengio, 2007; Tsuchida et al., 2018, 2019a; Pearce et al., 2019; Tsuchida et al., 2019b), although some of these require $\boldsymbol{\mu} = \mathbf{0}$. Most notably, the kernel is known for historically relevant activation functions $\psi(z) = \text{erf}(z)$ and RBF networks (Williams, 1997) and for the more modern ReLU activation, $\psi(z) = \max(0, z)$ (Cho and Saul, 2009).

1.1.2 Extensions

Once the form of the kernel (1) is known, the kernel of deep networks can be evaluated in the case where $\Sigma = \text{diag}(\sigma_w^2, \dots, \sigma_w^2, \sigma_d^2)$ and $\boldsymbol{\mu} = \mathbf{0}$ (Matthews et al., 2018; Lee et al., 2018; Yang, 2019a,b). The case where $\boldsymbol{\mu} \neq \mathbf{0}$ can also be handled (Tsuchida et al., 2019b), but we focus on $\boldsymbol{\mu} = \mathbf{0}$ in this work. The kernel in layer $l+1$ can be found iteratively² as a function of the kernel in layer l through

$$k^{(l+1)}(\mathbf{x}_1, \mathbf{x}_2) = \sigma_w^2 \mathbb{E} \left[\psi(s_1^{(l)} Z_1) \psi(s_2^{(l)} Z_2) \right] + \sigma_b^2, \\ (Z_1, Z_2)^\top \sim \mathcal{N} \left(\mathbf{0}, \begin{bmatrix} 1 & \cos\theta^{(l)} \\ \cos\theta^{(l)} & 1 \end{bmatrix} \right), \quad (2)$$

where $\cos\theta^{(l)}$ is the normalised kernel in layer l , and $s_i^{(l)} = \sqrt{k^{(l)}(\mathbf{x}_i, \mathbf{x}_i)}$.

²The $\boldsymbol{\mu} \neq \mathbf{0}$ formulation also requires iterating a mean-like function in addition to the kernel.

Definition 2. We call $k^{(l)}$ in (2) the kernel in layer l and $\cos\theta^{(l)} = \frac{k^{(l)}(\mathbf{x}_1, \mathbf{x}_2)}{\sqrt{k^{(l)}(\mathbf{x}_1, \mathbf{x}_1)k^{(l)}(\mathbf{x}_2, \mathbf{x}_2)}}$ the normalised kernel in layer l .

A generalisation of iid weight priors to partially exchangeable weight priors is also available (Tsuchida et al., 2019b), resulting in a GP with an additional layer of inference over the hyperparameters $\boldsymbol{\mu}$ and Σ .

Convergence to GPs also occurs for other neural network architectures such as convolutional architectures (Garriga-Alonso et al., 2018; Novak et al., 2019) and general compositions of recurrent, graph convolution, pooling, skip connection, attention and normalisation layers (Yang, 2019a,b).

1.1.3 Fixed points of kernel iteration

It is interesting to study the fixed-point dynamics of the normalised kernel, with applications to both GPs and finite-width networks. For example, it is known that when ψ is LReLU, the normalised kernel has a unique fixed point at $\cos\theta = 1$ (Tsuchida et al., 2018). We will make this more precise and provide an alternative proof as a consequence of our main theorem in § 4.3. The existence of a unique fixed point at $\cos\theta = 1$ says two interesting things, one about GPs with deep kernels and one about finite-width MLPs.

1. When applied to GPs, the covariance function of deep networks is approximately constant on hyperspheres of constant $\|\mathbf{x}\|$, and so function draws from the prior are almost constant. Therefore, increasingly deep kernels of this form represent a strict and potentially undesirable prior.
2. When applied heuristically to finite-width networks, the fixed point has an interesting geometric interpretation. No matter the angle between \mathbf{x}_1 and \mathbf{x}_2 of the same norm, the angle between the signals in deep layers of random iid networks is approximately zero, resulting in approximately input-independent (constant) outputs.

The overarching goal in this paper is to study the fixed point dynamics of (2) for general ψ . In particular, we are interested in avoiding unique fixed points which lead to undesirable input-independence.

1.1.4 New activation functions

The increased volume of gradient-based deep learning research has seen the introduction of new popular activation functions. Notably these include the exponential linear unit (ELU) (Clevert et al., 2016), the Gaussian error linear unit (GELU) (Hendrycks and

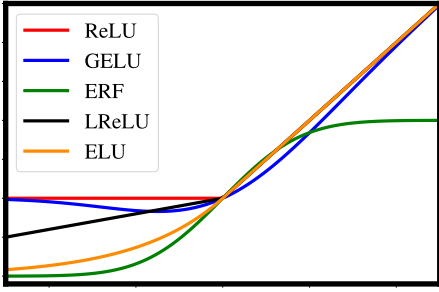


Figure 1: Visual comparison of different ψ .

Gimpel, 2016) and the Swish (Ramachandran et al., 2017; Elfwing et al., 2018).

Many state-of-the-art models use GELU (Radford et al.; Devlin et al., 2019) or swish activations (Chua et al., 2018). However, even when critically evaluating empirical evidence, it is difficult to determine whether certain activation functions are a better choice for a given problem, let alone separate the activation function expressivity from the ability of optimisers to find good solutions. Analysing activation functions through the lens of GPs (or more generally, kernel methods) allows one to visualise the function space in isolation of the ability of the optimiser to find good solutions.

1.2 Contributions

This paper contains two main contributions.

1. The GELU and ELU activation functions shown in Figure 1 are given by

$$\begin{aligned}\psi(z) &= z\Phi(z) \quad \text{and} \\ \psi(z) &= \Theta(z)z + \Theta(-z)(e^z - 1)\end{aligned}$$

respectively, where Φ denotes the CDF of the standard Gaussian and Θ denotes the Heaviside step function. We derive kernels for both cases and verify our results numerically. We compare the performance of GPs with different neural network kernels on some benchmarks.

2. We study the fixed point dynamics of the kernel when ψ is bounded by the absolute value of a polynomial. We find sufficient conditions for the existence of a unique fixed point of (2). We show theoretically and empirically that unlike the kernel corresponding to ReLU ψ , the new kernels are able to avoid unique fixed points.

1.3 Notation

We use \mathbf{x}_1 and \mathbf{x}_2 to denote two (not necessarily distinct) vectors in \mathbb{R}^d , $d < \infty$, each serving as inputs to a network layer. We denote the Euclidean norm by $\|\cdot\|$.

$\Theta : \mathbb{R} \rightarrow \{0, 1/2, 1\}$ denotes the Heaviside step function mapping negative numbers to 0, positive numbers to 1, and 0 to 1/2. The PDF and CDF of the standard normal distribution are denoted by ϕ and Φ respectively. The error function $\frac{2}{\sqrt{2\pi}} \int_0^z e^{-x^2} dx$ is denoted by $\text{erf} : \mathbb{R} \rightarrow (-1, 1)$.

We let $\mathbf{Z} = (Z_1, Z_2)^\top \sim \mathcal{N}(\mathbf{0}, S)$, with S having diagonal and off-diagonal elements 1 and $\rho = \cos\theta$ respectively.

2 The GELU kernel

In the same spirit as Williams (1997), we introduce dummy parameters β_1 and β_2 in the argument of Φ and then differentiate with respect to β_1 and β_2 to obtain a PDE. We then solve the PDE and evaluate the solution at $\beta_1 = \beta_2 = 1$.

Proposition 3. *When ψ is the GELU and $\mu = 0$, the kernel (1) is given by the equation in Figure 2.*

Complete working is given in Appendix A. It is plausible that our method of derivation extends to the case $\mu \neq 0$, although the calculations and resulting expression become more complicated. Even with $\mu = 0$, this kernel has some interesting properties that we discuss in § 4.

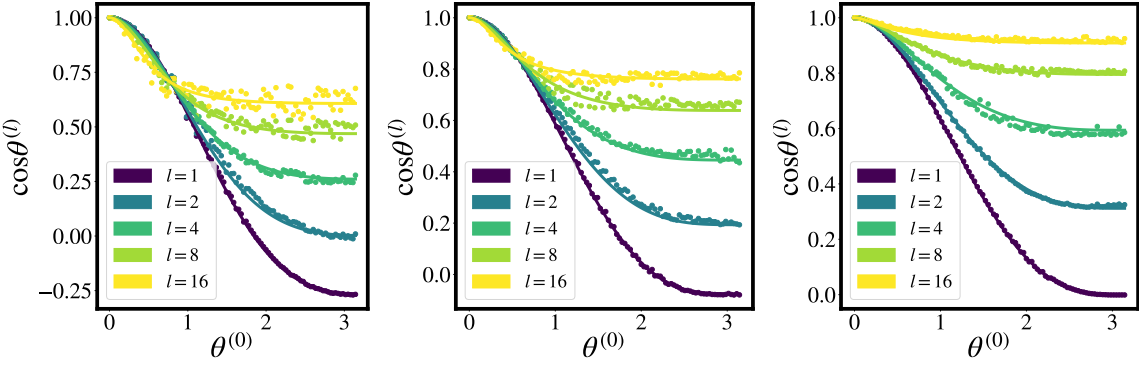
Interestingly, unlike the ELU kernel with $\mu = 0$, the GELU kernel does not contain any hard-to-compute special functions, only some (inverse) trigonometric functions.

3 The ELU kernel

Our expression is lengthy and we do not assemble it in the main text, but provide a visualisation in the form of Figure 3.

Proposition 4. *When ψ is the ELU, the kernel (1) has an analytical expression implemented in software¹ in terms of the univariate and bivariate normal CDFs.*

Complete working is given in Appendix B. Unfortunately, the ELU kernel involves exponentiating arguments involving s_1 and s_2 . This can lead to numerical instability in GP regression when many data points are involved. Despite this, having an analytical expression still allows us to gain insights into finite width networks, as we shall see in § 4.



$$k(\mathbf{x}_1, \mathbf{x}_2) = \sigma_b^2 + \sigma_w^2$$

$$\left(\frac{s_1^2 s_2^2}{2\pi} \left[\frac{\frac{1}{2}(\cos(2\theta) + 3) + s_1^2 + s_2^2 + s_1^2 s_2^2 \sin^2 \theta}{(1 + s_1^2)(1 + s_2^2) \sqrt{1 + s_1^2 + s_2^2 + s_1^2 s_2^2 \sin^2 \theta}} + \cos \theta \tan^{-1} \left(\frac{\cos \theta s_1 s_2}{\sqrt{1 + s_1^2 + s_2^2 + s_1^2 s_2^2 \sin^2 \theta}} \right) \right] + \frac{s_1 s_2}{4} \cos \theta \right).$$

Figure 2: The GELU kernel. The plots show the normalised kernels in layer l as a function of the angle $\theta^{(0)}$ between the inputs for MLPs of increasing depth when $\Sigma = \text{diag}(\sigma_w^2, \dots, \sigma_w^2, 0)$ and $\|\mathbf{x}_i\|$ is constant for all i . Values of σ_w are chosen specifically to preserve the expected square norm $\|\mathbf{x}\|^2$. Solid curve shows infinitely wide limit, and dots show samples from a network with 2 inputs and 3000 neurons in each layer. Each dot corresponds to a \mathbf{x}_1 and \mathbf{x}_2 generated through a random rotation of $(1, 0)^\top$ and $(\cos \theta^{(0)}, \sin \theta^{(0)})^\top$. The random rotation is generated through a QR decomposition of a matrix containing entries generated independently from the uniform distribution on $[0, 1]$. (Left) $\|\mathbf{x}\| = 0.5$, $\sigma_w = 1.591$ (Middle) $\|\mathbf{x}\| = 1$, $\sigma_w = 1.468$. (Right) $\|\mathbf{x}\| = 5$, $\sigma_w = 1.415$.

4 Fixed point analysis

For the remainder of the paper, we suppose all the weights have the same variance, and so do all the biases. That is, the first d diagonal entries of the diagonal matrix Σ are σ_w^2 , and the last diagonal entry is σ_b^2 .

4.1 Warm-up — norm preservation

One useful application of the kernel in finite-width iid-initialised networks is to track the expected squared norm of the signal in each layer given the norm in the previous layer as the depth of the network increases. This is important in weight initialisation of networks trained using gradient based optimisers to avoid exploding or vanishing signals.

The expected norm squared of the signal in the first hidden layer is $(k^{(1)}(\mathbf{x}_1, \mathbf{x}_1) - \sigma_b^2)/\sigma_w^2$. If we want the squared norm of the signal in the hidden layer to be the same as the squared norm of the input, we set $\|\tilde{\mathbf{x}}_1\|^2 = (k^{(1)}(\mathbf{x}_1, \mathbf{x}_1) - \sigma_b^2)/\sigma_w^2$. We may then solve this condition to find the hyperparameter values that preserve input norms. For example, using the kernel corresponding to ReLU (Cho and Saul, 2009), one obtains He initialisation (He et al., 2015), that $\sigma_w = \sqrt{2}$, where $\Sigma^{1/2} = \text{diag}(\sigma_w, \dots, \sigma_w, 0)^\top$.

The analogue for GELU is more involved in the sense that no single σ_w will preserve the expected square norms of all input signals. Setting $\sigma_b = 0$, $k(\mathbf{x}, \mathbf{x})/\sigma_w^2 = \|\mathbf{x}\|^2$ and $s_1 = s_2 = \sigma_w \|\mathbf{x}\|$ in the equation in Figure 2, we would like to find a root $\sigma^*(\|\mathbf{x}\|)$ of

$$g_{\|\mathbf{x}\|}(\sigma) = \frac{\sigma^4 \|\mathbf{x}\|^2}{\pi(\sigma^2 \|\mathbf{x}\|^2 + 1) \sqrt{2\sigma^2 \|\mathbf{x}\|^2 + 1}} + \frac{\sigma^2}{4} \left(1 + \frac{2}{\pi} \sin^{-1} \frac{\sigma^2 \|\mathbf{x}\|^2}{1 + \sigma^2 \|\mathbf{x}\|^2} \right) - 1.$$

The root can be found numerically using an appropriate root-finding method. Figure 4 shows a plot of $\sigma^*(\|\mathbf{x}\|)$ as $\|\mathbf{x}\|$ varies. It is straightforward to show that root of the limit of $g_{\|\mathbf{x}\|}(\sigma)$ as $\|\mathbf{x}\| \rightarrow \infty$ is $\sqrt{2}$, which interestingly recovers He initialisation. This implies that when data has large norms (such as images or audio files), He initialisation is suitable.

The same procedure can be carried out for the ELU kernel, and the roots are also shown in Figure 4. This procedure may be viewed as a warm-up handling the special case of $\mathbf{x}_1 = \mathbf{x}_2$ for our more general fixed point analysis.

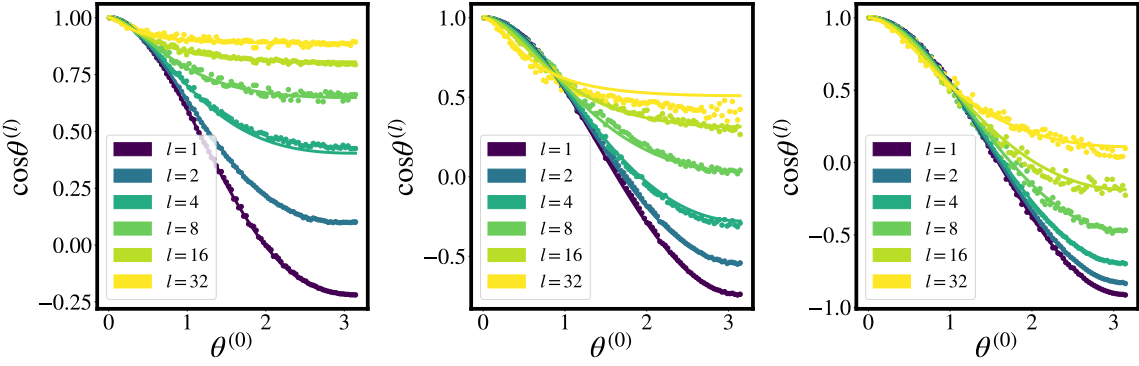


Figure 3: As in Figure 2, but with ELU ψ . (Left) $\|\mathbf{x}\| = 5, \sigma = 1.40$ (Middle) $\|\mathbf{x}\| = 1, \sigma = 1.27$. (Right) $\|\mathbf{x}\| = 0.5, \sigma = 1.17$.

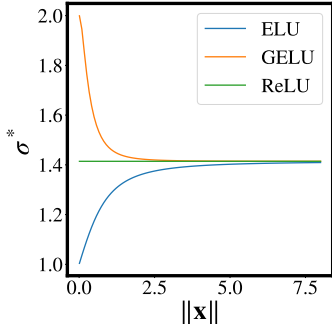


Figure 4: Values of σ that preserve the layer-wise expected square norm of $\|\mathbf{x}\|$ in MLPs with GELU, ELU and ReLU activations.

4.2 General fixed point analysis

Let $\mathcal{S} \subseteq [0, \infty) \times [0, \infty) \times [-1, 1]$. In the infinitely wide limit, we may view each layer as updating a state $(s_1^2, s_2^2, \cos \theta) \in \mathcal{S}$ through a function $\mathbf{g} : \mathcal{S} \rightarrow \mathcal{S}$. In this section, we analyse the fixed point behaviour of \mathbf{g} .

Let $(G_1, G_2)^\top \sim \mathcal{N}(\mathbf{0}, I)$. We are interested in the fixed-point dynamics of the iterated map \mathbf{g} having components

$$\begin{aligned} g_1(s_1^2, s_2^2, \rho) &= \sigma_w^2 \mathbb{E}[\psi^2(s_1 G_1)] + \sigma_b^2 \\ g_2(s_1^2, s_2^2, \rho) &= \sigma_w^2 \mathbb{E}[\psi^2(s_2 G_2)] + \sigma_b^2 \\ g_3(s_1^2, s_2^2, \rho) &= \frac{\mathbb{E}[\sigma_w^2 \psi(s_1 G_1) \psi(s_2 (G_1 \rho + G_2 \sqrt{1 - \rho^2})) + \sigma_b^2]}{\sqrt{g_1 g_2}}, \end{aligned} \quad (3)$$

which track the expected square norms (after a linear transformation involving σ_w^2 and σ_b^2) and normalised kernel as the signals propagate through the layers³.

³In the numerator of g_3 , we expressed the kernel (1) in terms of iid Gaussians \mathbf{G} instead of dependent Gaussians \mathbf{Z} .

By inspection, g_3 (but not necessarily \mathbf{g}) always has an uncountable set of fixed points at $\rho = 1$ along $s_1 = s_2$. Banach's fixed point theorem says that if \mathbf{g} is a contraction mapping on \mathcal{S} , then \mathbf{g} has a unique fixed point in \mathcal{S} (Agarwal et al., 2001).

Theorem 5. *Let (\mathcal{S}, d) be a complete metric space. A function $\mathbf{g} : \mathcal{S} \rightarrow \mathcal{S}$ is a contraction mapping if there exists some $0 \leq c < 1$ satisfying $d(\mathbf{g}(\mathbf{r}_1), \mathbf{g}(\mathbf{r}_2)) \leq c d(\mathbf{r}_1, \mathbf{r}_2)$ for all $\mathbf{r}_1, \mathbf{r}_2 \in \mathcal{S}$.*

Let $\mathbf{g} : \mathcal{S} \rightarrow \mathcal{S}$ be a contraction mapping. Then \mathbf{g} admits a unique fixed point $\mathbf{r}^ \in \mathcal{S}$ satisfying $\mathbf{g}(\mathbf{r}^*) = \mathbf{r}^*$ and $\mathbf{r}^* = \lim_{n \rightarrow \infty} \mathbf{g}^n(\mathbf{r}_0)$ for some arbitrary element $\mathbf{r}_0 \in \mathcal{S}$.*

To this end, we study the eigenvalues of the Jacobian of \mathbf{g} ; \mathbf{g} is a contraction mapping with respect to the Euclidean norm if the eigenvalues are strictly less than 1.

We are interested in studying expectations of objects that may not be integrable functions with respect to the Gaussian measure, namely *tempered distributions*. In order to do so, we denote the set of Schwartz functions on the plane by $D(\mathbb{R}^2)$ and its dual space, the space of tempered distributions, by $D'(\mathbb{R}^2)$, and observe that $\phi \in D(\mathbb{R}^2)$. For $q \in D(\mathbb{R}^2)$ and $T \in D'(\mathbb{R}^2)$, write $\langle T, q \rangle$ for the dual pairing of T and q .

For any $q \in D(\mathbb{R}^2)$ we can then define an operator q^* on $D'(\mathbb{R}^2)$ via the natural injection into the dual space of $D'(\mathbb{R}^2)$ by setting $q^*(T) = \langle T, q \rangle$ for any $T \in D'(\mathbb{R}^2)$. We can then define the expectation of the distribution by defining $\mathbb{E}[T] = \langle T, \phi \rangle$, which agrees with the usual definition whenever T can be represented by an integrable function.

Following Jones (1982), we define the derivative of a tempered distribution via $\langle \frac{\partial}{\partial x} T, q \rangle = -\langle T, \frac{\partial}{\partial x} q \rangle$, and when T can be represented by a locally integrable function f , we abuse notation to write $\int_{\mathbb{R}^2} \frac{\partial f}{\partial x} \phi :=$

$-\int_{\mathbb{R}^2} f \frac{\partial \phi}{\partial x}$. This is analogously extended for higher order derivatives by ensuring integration by parts holds whenever f is smooth.

Theorem 6. *Let \mathbf{g} be as in (3), and suppose the absolute value of ψ is bounded by a polynomial. Let $(Z_1, Z_2) \sim \mathcal{N}(\mathbf{0}, S)$ with covariance $\rho = \cos \theta$ and unit variances. Then for $\rho \in (-1, 1)$ $0 < s_1, s_2$, the (unordered) eigenvalues of the Jacobian of \mathbf{g} are*

$$\begin{aligned}\lambda_1 &= \sigma_w^2 \mathbb{E}[\psi(s_1 Z_1) \psi'(s_1 Z_1) Z_1] / s_1, \\ \lambda_2 &= \sigma_w^2 \mathbb{E}[\psi(s_2 Z_2) \psi'(s_2 Z_2) Z_2] / s_2, \quad \text{and} \\ \lambda_3 &= \frac{\sigma_w^2 s_1 s_2}{\sqrt{g_1 g_2}} \mathbb{E}[\psi'(s_1 Z_1) \psi'(s_2 Z_2)],\end{aligned}$$

provided the right hand terms are finite, where ψ' is the distributional derivative of ψ .

Proof. We begin by evaluating the derivative of g_3 with respect to ρ . Note that the mapping $T_\psi : D(\mathbb{R}^2) \rightarrow \mathbb{R}$ satisfying

$$T_\psi(q) = \int \psi(s_1 \omega_1) \psi(s_2(\omega_1 \rho + \omega_2 \sqrt{1 - \rho^2})) q(\omega) d\omega$$

is a tempered distribution since for all $q \in D(\mathbb{R}^2)$,

$$\begin{aligned}&\int |\psi(s_1 \omega_1) \psi(s_2(\omega_1 \rho + \omega_2 \sqrt{1 - \rho^2})) q(\omega)| d\omega \\ &\leq \int p(\omega) |q(\omega)| d\omega < \infty,\end{aligned}$$

where p is some polynomial. Differentiating g_3 with respect to ρ we find

$$\begin{aligned}\frac{\partial g_3}{\partial \rho} &= \sigma_w^2 \frac{\partial}{\partial \rho} \langle T_\psi, \phi_\rho \rangle / \sqrt{g_1 g_2} \\ &= \sigma_w^2 \mathbb{E}[\psi(s_1 G_1) \psi'(s_2(G_1 \rho + G_2 \sqrt{1 - \rho^2})) \\ &\quad (G_1 - G_2 \cot \theta) s_2] / \sqrt{g_1 g_2}.\end{aligned}$$

Let (Z_1, Z_2, Z_3) be multivariate Gaussian, each element having zero mean, unit variance and correlation structure $\mathbb{E}[Z_1 Z_2] = \rho$, $\mathbb{E}[Z_1 Z_3] = 0$, and $\mathbb{E}[Z_3 Z_2] = \sin \theta$. Then

$$\frac{\partial g_3}{\partial \rho} = \frac{\sigma_w^2 s_2}{\sqrt{g_1 g_2}} \mathbb{E}[\psi(s_1 Z_1) \psi'(s_2 Z_2) (Z_1 - Z_3 \cot \theta)].$$

Two applications of a multivariate version of Stein's lemma for tempered distributions (Lemma 9 in Appendix C) yield

$$\begin{aligned}\frac{\partial g_3}{\partial \rho} &= \frac{\sigma_w^2 s_2}{\sqrt{g_1 g_2}} \left[s_1 \mathbb{E}[\psi'(s_1 Z_1) \psi'(s_2 Z_2)] + \right. \\ &\quad \left. \rho s_2 \mathbb{E}[\psi(s_1 Z_1) \psi''(s_2 Z_2)] - \right. \\ &\quad \left. \rho s_2 \mathbb{E}[\psi(s_1 Z_1) \psi''(s_2 Z_2)] \right] \\ &= \frac{\sigma_w^2 s_1 s_2}{\sqrt{g_1 g_2}} \mathbb{E}[\psi'(s_1 Z_1) \psi'(s_2 Z_2)].\end{aligned}$$

Finally, note g_3 is infinitely differentiable in ρ on $(-1, 1)$ (see Appendix D).

The Jacobian is triangular, and the other diagonal entries may be evaluated by analogous calculations to the above, without the need for Stein's lemma. The eigenvalues of the Jacobian are simply its diagonal elements. \square

Remark 7. *One may consider two simplified cases involving a reduced state-space with only g_3 updating ρ . Suppose $\sigma_b^2 = 0$ (as is common when initialising neural networks).*

1. *If ψ is absolutely homogeneous ($\psi(|a|z) = |a|\psi(z)$, which also implies $\psi'(|a|z) = \psi'(z)$), then*

$$\frac{\partial g_3}{\partial \rho} = \lambda_3 = \frac{\mathbb{E}[\psi'(Z_1) \psi'(Z_2)]}{\mathbb{E}[\psi^2(Z_1)]},$$

which does not depend on σ_w .

2. *If a fixed point of the system only involving s_1 and g_1 exists at a value $\sigma_w = \sigma^*$ and $s_1 = s_2 = s$ at the fixed point, we have*

$$\frac{\partial g_3}{\partial \rho} = \lambda_3 = (\sigma^*)^2 \mathbb{E}[\psi'(s Z_1) \psi'(s Z_2)].$$

Note that our result does not include $\rho \in \{-1, 1\}$. With the additional assumption that ψ is continuous almost everywhere, the expression for λ_3 is valid on the closed interval $\rho \in [-1, 1]$, as shown in Appendix E.

4.3 Example, ReLU

The ReLU, along with Leaky ReLU (LReLU), PReLU and absolute value activations, falls into the first case of Remark 7. Then

$$\lambda_3 = \frac{dg_3}{d\rho} = \frac{\mathbb{E}[\psi'(Z_1) \psi'(Z_2)]}{\mathbb{E}[\psi^2(Z_1)]} = \frac{1}{\pi}(\pi - \theta),$$

where the last equality is due to Sheppard's identity (Sheppard, 1899; O'Donnell, 2014), or can be otherwise evaluated (Cho and Saul, 2009). By Theorem 5, this system contains a unique fixed point at $\rho = 1$. For g_1 and g_2 to have fixed points, we do require that $\sigma_w \leq \sqrt{2}$, where equality preserves the expected squared norm and inequality shrinks the expected squared norm to 0. It can be shown that the same fixed point holds for LReLU and absolute value activations (Tsuchida et al., 2018).

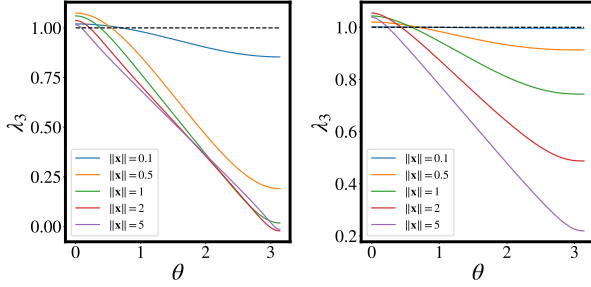


Figure 5: Eigenvalues λ_3 for (Left) GELU (Right) ELU.

4.4 Example, GELU

We consider the dynamics on a ball of constant $\|\mathbf{x}\|$, where σ_w is chosen such that $g_1 = \|\mathbf{x}\|$ (as in Figure 4). This corresponds to case 2 of Remark 7. λ_3 is the sum of

$$\begin{aligned} & \sigma_w^2 \mathbb{E} \left[\Phi(\sigma_w \|\mathbf{x}\| Z_1) \Phi(\sigma_w \|\mathbf{x}\| Z_2) \right] \\ &= \frac{\sigma_w^2}{4} \left(1 + \frac{2}{\pi} \sin^{-1} \frac{\sigma_w^2 \|\mathbf{x}\|^2 \cos \theta}{1 + \sigma_w^2 \|\mathbf{x}\|^2} \right), \end{aligned}$$

due to Williams (1997),

$$\begin{aligned} & 2\sigma_w^2 \mathbb{E} \left[\Phi(\sigma_w \|\mathbf{x}\| Z_1) (\sigma_w \|\mathbf{x}\| Z_2) \phi(\sigma_w \|\mathbf{x}\| Z_2) \right] \\ &= \frac{\sigma_w^4 \|\mathbf{x}\|^2 \cos \theta}{\pi(\sigma_w^2 \|\mathbf{x}\|^2 + 1) \sqrt{\sigma_w^4 \|\mathbf{x}\|^4 \sin^2 \theta + 2\sigma_w^2 \|\mathbf{x}\|^2 + 1}} \end{aligned}$$

by introducing a dummy parameter into Φ and obtaining an initial value problem, and

$$\begin{aligned} & \sigma_w^2 \mathbb{E} \left[(\sigma_w \|\mathbf{x}\| Z_1) \phi(\sigma_w \|\mathbf{x}\| Z_1) (\sigma_w \|\mathbf{x}\| Z_2) \phi(\sigma_w \|\mathbf{x}\| Z_2) \right] \\ &= \frac{\sigma_w^4 \|\mathbf{x}\|^2 \cos \theta}{2\pi(1 + 2\sigma_w^2 \|\mathbf{x}\|^2 + \sigma_w^4 \|\mathbf{x}\|^4 \sin^2 \theta)^{3/2}} \end{aligned}$$

by combining the products of ϕ in the integral definition of expectation. Full working is given in Appendix F.1.

4.5 Example, ELU

We may evaluate the eigenvalue corresponding to case 2 of Remark 7. λ_3 is the sum of

$$\sigma_w^2 \mathbb{E} [\Theta(\sigma_w \|\mathbf{x}\| Z_1) \Theta(\sigma_w \|\mathbf{x}\| Z_2)] = \frac{\sigma_w^2}{2\pi} (\pi - \theta)$$

by Sheppard's identity,

$$\begin{aligned} & 2\sigma_w^2 \mathbb{E} [\Theta(\sigma_w \|\mathbf{x}\| Z_1) \Theta(-\sigma_w \|\mathbf{x}\| Z_2) e^{\sigma_w \|\mathbf{x}\| Z_2}] \\ &= 2\sigma_w^2 e^{\sigma_w^2 \|\mathbf{x}\|^2 / 2} \Phi(-\sigma_w \|\mathbf{x}\|, \sigma_w \|\mathbf{x}\| \cos \theta; -\cos \theta) \end{aligned}$$

by completing the square inside the exponential, and

$$\begin{aligned} & \sigma_w^2 \mathbb{E} [\Theta(-\sigma_w \|\mathbf{x}\| Z_1) \Theta(-\sigma_w \|\mathbf{x}\| Z_2) e^{\sigma_w \|\mathbf{x}\| Z_2 + \sigma_w \|\mathbf{x}\| Z_1}] \\ &= \sigma_w^2 e^{\sigma_w \|\mathbf{x}\|^2 (1 + \cos \theta)} \\ & \Phi(-\sigma_w \|\mathbf{x}\| (1 + \cos \theta), -\sigma_w \|\mathbf{x}\| (1 + \cos \theta); \cos \theta), \end{aligned}$$

by again completing the square inside the argument of the exponential. Full working is given in Appendix F.2.

For both the GELU and ELU, we evaluate $\lambda_3(\theta)$ at the location $(\sigma^*(\|\mathbf{x}\|), \|\mathbf{x}\|)$ for different values of $\|\mathbf{x}\|$ in Figure 5. We observe that each exceeds 1 on the interval, and is therefore not a contraction mapping hence not guaranteed to have a unique fixed point. This is consistent with Figures 2 and 3, where fixed points are shown by intersecting curves.

5 Gaussian process experiments

We compare the performance of GP regression models using ReLU, LReLU, ERF and GELU kernels on a popular Bayesian deep learning benchmark (Hernández-Lobato and Adams, 2015). All data was standardised to have 0 mean and unit variance. The ELU kernel was not included in our experiments, as discussed in § 3. We split our experimental analysis into two sections, shallow models having a single hidden layer, and deep models having up to 32 layers.

5.1 Shallow models

How do differences in priors over functions induced by various activation functions affect empirical performance? Using the limiting GP allows us to remove the interaction between ψ and optimisation, and purely consider the effect of ψ on the functional prior.

Figure 7 shows the predictive distribution of GPs with GELU, ReLU, LReLU and ERF kernels on a toy regression task. ERF has different extrapolation properties due to being a bounded activation, whilst the others appear qualitatively similar, though with extrapolation variance decreasing in the order GELU/ReLU/LReLU.

Figure 6 shows the benchmark results for single-hidden-layer GPs fitted on 90% of the data with negative log likelihood (NLL) and RMSE computed over the remaining 10%. See Appendix G.1 for details. All kernels achieve comparable accuracy, but small gains can be achieved by selecting a kernel suited to the dataset. Results are most different for ERF — either negatively (Concrete, Energy) or positively (Boston, Protein, Wine). Interestingly, on some datasets, differences are also observed between GELU/ReLU/LReLU. For example, GELU offers an advantage in Naval and Yacht, and LReLU performs poorly on Protein.

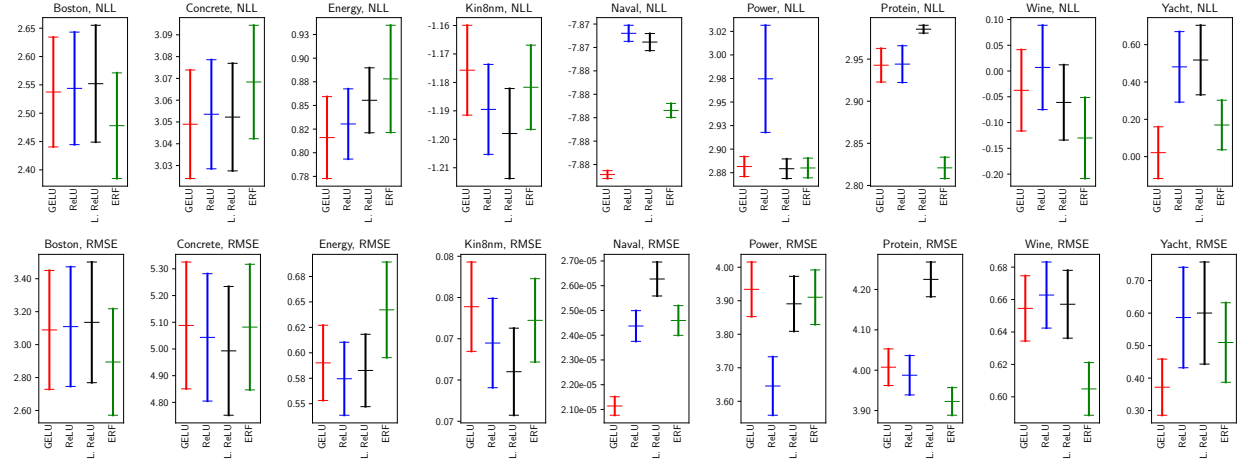


Figure 6: NLL and RMSE for equivalent single layer GPs. Mean ± 2 standard errors (over 20 runs).

Table 1: Best performing models for each kernel over the grid search.

	ReLU			GELU			LReLU			ERF		
	RMSE	σ_w^2	ℓ	RMSE	σ_w^2	ℓ	RMSE	σ_w^2	ℓ	RMSE	σ_w^2	ℓ
Boston	2.85 ± 0.64	1.90	7	2.86 ± 0.65	1.80	6	2.60 ± 1.07	2.00	32	2.69 ± 0.95	5.00	2
Concrete	5.22 ± 0.55	5.00	2	5.21 ± 0.56	5.00	2	5.23 ± 0.44	3.30	3	5.63 ± 0.46	5.00	2
Energy	0.89 ± 0.11	5.00	2	0.92 ± 0.12	5.00	2	2.77 ± 0.31	0.10	1	2.79 ± 0.23	0.10	1
Wine	1.15 ± 0.13	5.00	4	1.17 ± 0.14	5.00	4	1.04 ± 0.12	5.00	5	3.96 ± 0.75	5.00	1
Yacht	0.58 ± 0.01	4.80	32	0.58 ± 0.01	2.30	32	0.60 ± 0.02	1.80	29	0.57 ± 0.02	5.00	8

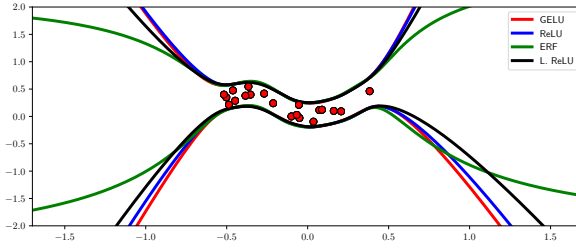


Figure 7: Predictive distribution (2 std. deviations) for GP kernels from equivalent single layer networks with various activation function on toy data.

These findings have implications for finite-width neural networks. They suggest that the difference in performance found by varying activation functions may partially derive from subtle differences in the induced prior over functions. This is in contrast to previously cited reasons such as bias shift and its relation to natural gradient (Clevert et al., 2016).

5.2 Deep models

How does the performance of models vary with depth?

We randomly shuffled the data 5 times into an 80%/20% train/test split. For each random shuffle, we ran GP regression with an additive iid Gaussian noise model having variance fixed at 0.1. We varied the depth ℓ and the weight and biases variances σ_w^2 in each layer, which were constrained to be equal. For each setting, we measured the RMSE between the mean of the GP prediction and the true regression targets. Figure 8 shows the average RMSE on the Wine dataset over 5 shuffles. We include plots of the other datasets in Appendix G.2. We make two qualitative observations. Firstly, deep models can sometimes out-perform shallow models. Secondly, the RMSE appears to change smoothly⁴ in both depth and σ_w^2 . Table 1 shows the best models obtained over the grid search for each kernel.

⁴The visual smoothness of plots is *not* due to averaging over 5 trials; smoothness is also observed when we plot results from only 1 random shuffling.

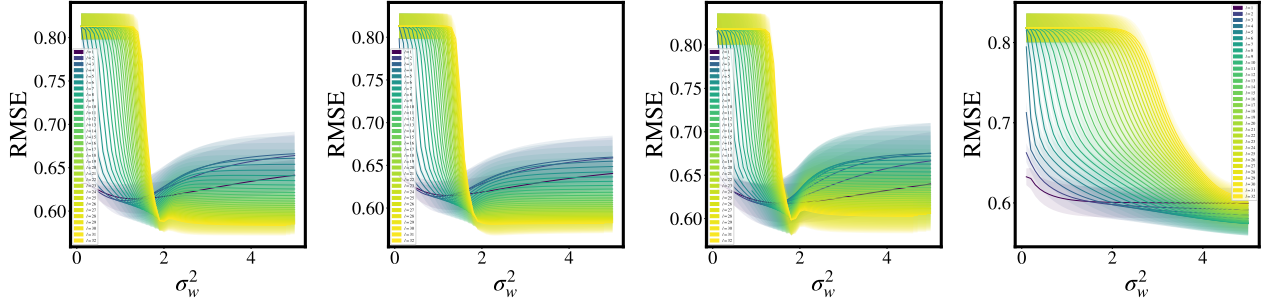


Figure 8: RMSE against σ_w^2 for the Wine dataset. Shaded region shows 1 standard deviation. (Left to Right) ReLU, GELU, LReLU, ERF.

6 Discussion

6.1 Relation to other work

Our work is closely related to earlier work (Schoenholz et al., 2017; Poole et al., 2016), with some important distinctions. They develop objects similar to $\frac{\partial g_3}{\partial \rho}$, but require bounded activations, and seem to also require some notion of differentiability. ReLU, LReLU, GELU and ELU activations do not fall into their analysis.

The neural tangent kernel (NTK) (Jacot et al., 2018) concerns the *training* dynamics of infinitely wide networks. Interestingly, the NTK has a form very similar to λ_3 . In future work, one could study fixed points in depth of the NTK, which would involve second distributional derivatives.

6.2 Conclusion

We introduced two new positive semi-definite kernels arising from the infinite-width limit of a one layer fully connected neural network having GELU and ELU activations. We provided visualisations of the kernel corresponding to networks of varying depths. We then introduced a general framework for understanding the fixed-point dynamics of such kernels. Using this framework, we showed theoretically that unlike the ReLU, the GELU and ELU kernels are able to avoid convergence to a unique fixed point. Empirically, our results are reflected in networks of finite-width.

We applied our new shallow and deep kernels in the setting of GP regression, finding that for some problems specific kernels are more appropriate, and that the new GELU kernel is competitive with the ReLU kernel.

References

Radford M Neal. *Bayesian learning for neural networks*. PhD thesis, University of Toronto, 1995.

Nicolas Le Roux and Yoshua Bengio. Continuous neural networks. In *Artificial Intelligence and Statistics*, pages 404–411, 2007.

Russell Tsuchida, Farbod Roosta-Khorasani, and Marcus Gallagher. Invariance of weight distributions in rectified MLPs. In *International Conference on Machine Learning*, pages 5002–5011, 2018.

Russell Tsuchida, Farbod Roosta-Khorasani, and Marcus Gallagher. Exchangeability and kernel invariance in trained MLPs. *International Joint Conference on Artificial Intelligence*, 2019a.

Tim Pearce, Russell Tsuchida, Mohamed Zaki, Alexandra Brintrup, and Andy Neely. Expressive priors in bayesian neural networks: Kernel combinations and periodic functions. *Uncertainty in Artificial Intelligence*, 2019.

Russell Tsuchida, Fred Roosta, and Marcus Gallagher. Richer priors for infinitely wide multi-layer perceptrons. *arXiv preprint arXiv:1911.12927*, 2019b.

Christopher KI Williams. Computing with infinite networks. In *Advances in neural information processing systems*, pages 295–301, 1997.

Youngmin Cho and Lawrence K. Saul. Kernel methods for deep learning. In *Advances in Neural Information Processing Systems*, pages 342–350. 2009.

Alexander G de G Matthews, Mark Rowland, Jiri Hron, Richard E Turner, and Zoubin Ghahramani. Gaussian process behaviour in wide deep neural networks. *The International Conference on Learning Representations*, 2018.

Jaehoon Lee, Yasaman Bahri, Roman Novak, Samuel S Schoenholz, Jeffrey Pennington, and Jascha Sohl-Dickstein. Deep neural networks as Gaussian processes. *The International Conference on Learning Representations*, 2018.

Greg Yang. Wide feedforward or recurrent neural networks of any architecture are gaussian processes. In *Advances in Neural Information Processing Systems*, pages 9947–9960. 2019a.

Greg Yang. Scaling limits of wide neural networks with weight sharing: Gaussian process behavior, gradient independence, and neural tangent kernel derivation. *arXiv preprint arXiv:1902.04760*, 2019b.

Adrià Garriga-Alonso, Carl Edward Rasmussen, and Laurence Aitchison. Deep convolutional networks as shallow Gaussian processes. *arXiv preprint arXiv:1808.05587*, 2018.

Roman Novak, Lechao Xiao, Jaehoon Lee, Yasaman Bahri, Greg Yang, Jiri Hron, Daniel A Abolafia, Jeffrey Pennington, and Jascha Sohl-Dickstein. Bayesian deep convolutional networks with many channels are gaussian processes. *The International Conference on Learning Representations*, 2019.

Djork-Arné Clevert, Thomas Unterthiner, and Sepp Hochreiter. Fast and accurate deep network learning by exponential linear units (ELUs). *The International Conference on Learning Representations*, 2016.

Dan Hendrycks and Kevin Gimpel. Gaussian error linear units (GELUs). *arXiv preprint arXiv:1606.08415*, 2016.

Prajit Ramachandran, Barret Zoph, and Quoc V Le. Searching for activation functions. *arXiv preprint arXiv:1710.05941*, 2017.

Stefan Elfwing, Eiji Uchibe, and Kenji Doya. Sigmoid-weighted linear units for neural network function approximation in reinforcement learning. *Neural Networks*, 107:3–11, 2018.

Alec Radford, Karthik Narasimhan, Tim Salimans, and Ilya Sutskever. Improving language understanding by generative pre-training. *Preprint. https://s3-us-west-2.amazonaws.com/openai-assets/research-covers/language-unsupervised/language_understanding_paper.pdf* (visited 2020-02-04).

J Devlin, M Chang, K Lee, and K Toutanova. Bert: Pre-training of deep bidirectional transformers for language understanding. In *Proceedings of the 2019 Conference of the North American Chapter of the Association for Computational Linguistics: Human Language Technologies*, pages 4171–4186, 2019.

Kurtland Chua, Roberto Calandra, Rowan McAllister, and Sergey Levine. Deep reinforcement learning in a handful of trials using probabilistic dynamics models. In *Advances in Neural Information Processing Systems*, pages 4754–4765, 2018.

Kaiming He, Xiangyu Zhang, Shaoqing Ren, and Jian Sun. Delving deep into rectifiers: Surpassing human-level performance on imagenet classification. In *Proceedings of the IEEE international conference on computer vision*, pages 1026–1034, 2015.

Ravi P Agarwal, Maria Meehan, and Donal O’regan.
Fixed point theory and applications, volume 141.
Cambridge university press, 2001.

D. S. Jones. *The theory of generalised functions*. Cambridge University Press, Cambridge ; New York, 2nd ed. edition, 1982.

William Fleetwood Sheppard. On the application of the theory of error to cases of normal distribution and normal correlation. *Philosophical Transactions of the Royal Society of London. Series A, Containing Papers of a Mathematical or Physical Character*, (192):140, 1899.

Ryan O’Donnell. *Analysis of boolean functions*, page 330. Cambridge University Press, 2014.

José Miguel Hernández-Lobato and Ryan P. Adams. Probabilistic Backpropagation for Scalable Learning of Bayesian Neural Networks. In *Proceedings of the 32nd International Conference on Machine Learning*, 2015.

Samuel S Schoenholz, Justin Gilmer, Surya Ganguli, and Jascha Sohl-Dickstein. Deep information propagation. *International Conference on Learning Representations*, 2017.

Ben Poole, Subhaneil Lahiri, Maithra Raghu, Jascha Sohl-Dickstein, and Surya Ganguli. Exponential expressivity in deep neural networks through transient chaos. In D. D. Lee, M. Sugiyama, U. V. Luxburg, I. Guyon, and R. Garnett, editors, *Advances in Neural Information Processing Systems 29*, pages 3360–3368. 2016.

Arthur Jacot, Franck Gabriel, and Clément Hongler. Neural tangent kernel: Convergence and generalization in neural networks. In *Advances in neural information processing systems*, pages 8571–8580, 2018.

S Rosenbaum. Moments of a truncated bivariate normal distribution. *Journal of the Royal Statistical Society: Series B (Methodological)*, 23(2):405–408, 1961.

A Derivation of GELU kernel

We would like to evaluate the kernel (up to a scaling and offset)

$$k(\mathbf{x}_1, \mathbf{x}_2) = s_1 s_2 \mathbb{E} \left[Z_1 Z_2 \Phi(s_1 Z_1) \Phi(s_2 Z_2) \right].$$

We split our evaluation of the kernel into two cases, first when $\theta \in (0, \pi)$, and second when $\theta \in \{0, \pi\}$.

A.1 $\theta \in (0, \pi)$

We introduce dummy variables β_1, β_2 and define

$$\kappa(\beta_1, \beta_2) = s_1 s_2 \mathbb{E} \left[Z_1 Z_2 \Phi(\beta_1 s_1 Z_1) \Phi(\beta_2 s_2 Z_2) \right].$$

The mixed derivative $\frac{\partial^2 \kappa}{\partial \beta_1 \partial \beta_2}$ is

$$\begin{aligned} & s_1^2 s_2^2 \mathbb{E} \left[Z_1^2 Z_2^2 \phi(\beta_1 s_1 Z_1) \phi(\beta_2 s_2 Z_2) \right] \\ &= s_1^2 s_2^2 \int z_1^2 z_2^2 \phi(\beta_1 s_1 z_1) \phi(\beta_2 s_2 z_2) \phi_2(z_1, z_2) dz_1 dz_2. \end{aligned} \quad (4)$$

The product of the normal PDFs is given by

$$\frac{1}{2\pi \sin \theta} \left(\frac{1}{\sqrt{2\pi}} \right)^2 \exp \left(-\frac{1}{2} (\mathbf{z}^\top S^{-1} \mathbf{z} + \mathbf{z}^\top \beta \mathbf{z}) \right),$$

where $S^{-1} = \frac{1}{\sin^2 \theta} \begin{bmatrix} 1 & -\cos \theta \\ -\cos \theta & 1 \end{bmatrix}$ and $\beta = \begin{bmatrix} s_1^2 \beta_1^2 \\ 0 \\ s_2^2 \beta_2^2 \end{bmatrix}$. Now $S^{-1} + \beta$ is the inverse of a positive definite covariance matrix, with

$$S^{-1} + \beta = \frac{1}{\sin^2 \theta} \begin{bmatrix} 1 + s_1^2 \beta_1^2 \sin^2 \theta & -\cos \theta \\ -\cos \theta & 1 + s_2^2 \beta_2^2 \sin^2 \theta \end{bmatrix},$$

having determinant

$$\csc^4 \theta ((1 + s_1^2 \beta_1^2 \sin^2 \theta)(1 + s_2^2 \beta_2^2 \sin^2 \theta) - \cos^2 \theta)$$

and inverse

$$\begin{aligned} & ((1 + s_1^2 \beta_1^2 \sin^2 \theta)(1 + s_2^2 \beta_2^2 \sin^2 \theta) - \cos^2 \theta)^{-1} \\ & \sin^2 \theta \begin{bmatrix} 1 + s_2^2 \beta_2^2 \sin^2 \theta & \cos \theta \\ \cos \theta & 1 + s_1^2 \beta_1^2 \sin^2 \theta \end{bmatrix}. \end{aligned}$$

We may therefore write (4) as

$$\frac{s_1^2 s_2^2}{2\pi \sin \theta} \det(S^{-1} + \beta)^{-\frac{1}{2}} \mathbb{E}[U_1^2 U_2^2],$$

where $(U_1, U_2)^\top$ has covariance matrix $C = (S^{-1} + \beta)^{-1}$. The expectation $\mathbb{E}[U_1^2 U_2^2]$ has a known form, and is given by

$$\begin{aligned} \mathbb{E}[U_1^2 U_2^2] &= C_{11} C_{22} + 2C_{12}^2 \\ &= ((1 + s_1^2 \beta_1^2 \sin^2 \theta)(1 + s_2^2 \beta_2^2 \sin^2 \theta) - \cos^2 \theta)^{-2} \\ &\quad ((1 + s_1^2 \beta_1^2 \sin^2 \theta)(1 + s_2^2 \beta_2^2 \sin^2 \theta) + 2 \cos^2 \theta) \\ &\quad \sin^4 \theta. \end{aligned}$$

Finally,

$$\begin{aligned} \frac{\partial^2 \kappa}{\partial \beta_1 \partial \beta_2} &= \frac{\sin^5 \theta s_1^2 s_2^2}{2\pi} \\ &\quad \left[((1 + s_1^2 \beta_1^2 \sin^2 \theta)(1 + s_2^2 \beta_2^2 \sin^2 \theta) - \cos^2 \theta)^{-5/2} \right. \\ &\quad \left. ((1 + s_1^2 \beta_1^2 \sin^2 \theta)(1 + s_2^2 \beta_2^2 \sin^2 \theta) + 2 \cos^2 \theta) \right]. \end{aligned}$$

We also have the boundary conditions

$$\begin{aligned} \frac{\partial \kappa}{\partial \beta_1} \Big|_{\beta_2=0} &= \frac{\partial \kappa}{\partial \beta_2} \Big|_{\beta_1=0} = 0, \quad \text{and} \\ \kappa(0, 0) &= \frac{s_1 s_2}{4} \cos \theta. \end{aligned}$$

The solution to this PDE can be found by direct integration with integration constants due to the conditions. The solution evaluated at $\beta_1 = \beta_2 = 1$ is

$$\begin{aligned} & \frac{s_1^2 s_2^2}{2\pi} \left[\frac{\frac{1}{2}(\cos(2\theta) + 3) + s_1^2 + s_2^2 + s_1^2 s_2^2 \sin^2 \theta}{(1 + s_1^2)(1 + s_2^2) \sqrt{1 + s_1^2 + s_2^2 + s_1^2 s_2^2 \sin^2 \theta}} \right. \\ & \quad \left. + \cos \theta \tan^{-1} \left(\frac{\cos \theta s_1 s_2}{\sqrt{1 + s_1^2 + s_2^2 + s_1^2 s_2^2 \sin^2 \theta}} \right) \right] + \frac{s_1 s_2}{4} \cos \theta. \end{aligned}$$

A.2 $\theta \in \{0, \pi\}$

We may simply evaluate the result obtained on $(0, \pi)$ at 0 and π . To see this, observe that k is continuous with respect to θ on $[0, \pi]$. Firstly,

$$\begin{aligned} \psi(s_1 Z_1) \psi(s_2 Z_2) &\leq \max\{\psi^2(s_1 Z_1), \psi^2(s_2 Z_2)\} \\ &\leq \psi^2(s_1 Z_1) + \psi^2(s_2 Z_2), \end{aligned}$$

which has finite expectation. Let $G_1 \perp\!\!\!\perp G_2 \sim \mathcal{N}(0, 1)$. By dominated convergence,

$$\begin{aligned} & \lim_{\theta \rightarrow 0} k(\cos \theta) \\ &= \mathbb{E} \left[\lim_{\theta \rightarrow 0} \psi(s_1 G_1) \psi(s_2 (\cos \theta G_1 + \sqrt{1 - \cos^2 \theta} G_2)) \right] \\ &= \mathbb{E} [\psi(s_1 G_1) \psi(s_2 G_1)] \\ &= k(1), \end{aligned}$$

and similarly for the case $\theta \rightarrow \pi$.

B Derivation of ELU kernel

We would like to evaluate the kernel (up to a scaling and offset)

$$\mathbb{E} \left[\left(\Theta(\tilde{Z}_1 + \tilde{\mu}_1)(\tilde{Z}_1 + \tilde{\mu}_1) + \Theta(-\tilde{Z}_1 - \tilde{\mu}_1)(e^{\tilde{Z}_1 + \tilde{\mu}_1} - 1) \right) \right. \\ \left. \left(\Theta(\tilde{Z}_2 + \tilde{\mu}_2)(\tilde{Z}_2 + \tilde{\mu}_2) + \Theta(-\tilde{Z}_2 - \tilde{\mu}_2)(e^{\tilde{Z}_2 + \tilde{\mu}_2} - 1) \right) \right],$$

where $\tilde{Z}_i = s_i Z_i$. We may expand the expectation into the sum of

$$E_1 = \mathbb{E} \left[\Theta(\tilde{Z}_1 + \tilde{\mu}_1)(\tilde{Z}_1 + \tilde{\mu}_1) \Theta(\tilde{Z}_2 + \tilde{\mu}_2)(\tilde{Z}_2 + \tilde{\mu}_2) \right], \quad (5)$$

$$E_2 = \mathbb{E} \left[\Theta(\tilde{Z}_1 + \tilde{\mu}_1)(\tilde{Z}_1 + \tilde{\mu}_1) \Theta(-\tilde{Z}_2 - \tilde{\mu}_2)(e^{\tilde{Z}_2 + \tilde{\mu}_2} - 1) \right], \quad (6)$$

$$E_3 = \mathbb{E} \left[\Theta(\tilde{Z}_2 + \tilde{\mu}_2)(\tilde{Z}_2 + \tilde{\mu}_2) \Theta(-\tilde{Z}_1 - \tilde{\mu}_1)(e^{\tilde{Z}_1 + \tilde{\mu}_1} - 1) \right], \quad (7)$$

and

$$E_4 = \mathbb{E} \left[\Theta(-\tilde{Z}_1 - \tilde{\mu}_1)(e^{\tilde{Z}_1 + \tilde{\mu}_1} - 1) \Theta(-\tilde{Z}_2 - \tilde{\mu}_2)(e^{\tilde{Z}_2 + \tilde{\mu}_2} - 1) \right]. \quad (8)$$

In the following sections we evaluate each term in the sum. It suffices to evaluate the kernel on the open interval $(0, \pi)$ by the same argument as in § A.2.

B.1 E_1

The integral (5) is a non-trivial generalisation of the arc-cosine kernel of degree 1 (Cho and Saul, 2009) with $\mu \neq 0$, and is evaluated by Tsuchida et al. (2019b).

B.2 E_2 and E_3

The second integral (6) is

$$\frac{s_1}{2\pi \sin \theta} \int_{\mathbb{R}^2} \Theta(z_1 + \tilde{\mu}_1/s_1)(z_1 + \tilde{\mu}_1/s_1) \Theta(-z_2 - \tilde{\mu}_2/s_2) (e^{s_2 z_2 - \tilde{\mu}_2} - 1) \exp \left(-\frac{1}{2} \mathbf{z}^\top S^{-1} \mathbf{z} \right) dz_1 dz_2.$$

We may complete the square of the exponentiated terms,

$$\begin{aligned} & \exp \left(-\frac{1}{2} (\mathbf{z}^\top S^{-1} \mathbf{z} - 2s_2 z_2) \right) \\ &= \exp \left(-\frac{1}{2} \left((\mathbf{z} - s_2 S_{:,2})^\top S^{-1} (\mathbf{z} - s_2 S_{:,2}) - s_2^2 \right) \right), \end{aligned}$$

where $S_{:,2}$ denotes the second column of S . E_2 is then

$$\begin{aligned} & e^{-\tilde{\mu}_2 + s_2^2/2} s_1 \mathbb{E} \left[\Theta(Z_1 + s_2 \cos \theta + \tilde{\mu}_1/s_1) \right. \\ & \quad \left. (Z_1 + s_2 \cos \theta + \tilde{\mu}_1/s_1) \Theta(-Z_2 - s_2 - \tilde{\mu}_2/s_2) \right] - \\ & s_1 \mathbb{E} \left[\Theta(Z_1 + \tilde{\mu}_1/s_1)(Z_1 + \tilde{\mu}_1/s_1) \Theta(-Z_2 - \tilde{\mu}_2/s_2) \right]. \end{aligned}$$

Both of these expectations can be related to the first moment of the truncated standard bivariate normal distribution, which has a known form. Let (Y_1, Y_2) be distributed according to the standard bivariate normal distribution with correlation $-\cos \theta$, and let $h, k \in \mathbb{R}$.

Defining M for convenience as follows, Rosenbaum (1961) gives

$$\begin{aligned} & M(h, k) \\ &= \mathbb{E} \left[\Theta(Y_1 - h) Y_1 \Theta(Y_2 - k) \right] \\ &= \frac{1}{2\pi \sin \theta} \int_k^\infty \int_h^\infty z_1 \exp \left(-\frac{1}{2 \sin^2 \theta} (z_1^2 + 2 \cos \theta z_1 z_2 + z_2^2) \right) dz_1 dz_2 \\ &= \phi(h) \left(1 - \Phi \left(\frac{k + h \cos \theta}{\sin \theta} \right) \right) - \\ & \quad \cos \theta \phi(k) \left(1 - \Phi \left(\frac{h + k \cos \theta}{\sin \theta} \right) \right). \end{aligned}$$

Therefore,

$$\begin{aligned} & s_1 \mathbb{E} \left[\Theta(Z_1 + \tilde{\mu}_1/s_1)(Z_1 + \tilde{\mu}_1/s_1) \Theta(-Z_2 - \tilde{\mu}_2/s_2) \right] \\ &= s_1 \left(M \left(-\frac{\tilde{\mu}_1}{s_1}, \frac{\tilde{\mu}_2}{s_2} \right) + \frac{\tilde{\mu}_1}{s_1} \Phi \left(-\frac{\tilde{\mu}_1}{s_1}, \frac{\tilde{\mu}_2}{s_2}; -\cos \theta \right) \right), \end{aligned}$$

and

$$\begin{aligned} & \mathbb{E} \left[\Theta(Z_1 + s_2 \cos \theta + \tilde{\mu}_1/s_1)(Z_1 + s_2 \cos \theta + \tilde{\mu}_1/s_1) \right. \\ & \quad \left. \Theta(-Z_2 - s_2 - \tilde{\mu}_2/s_2) \right] \\ &= M \left(-s_2 \cos \theta - \frac{\tilde{\mu}_1}{s_1}, s_2 + \frac{\tilde{\mu}_2}{s_2} \right) + \\ & \quad \left(s_2 \cos \theta + \frac{\tilde{\mu}_1}{s_1} \right) \Phi \left(s_2 \cos \theta - \frac{\tilde{\mu}_1}{s_1}, -s_2 + \frac{\tilde{\mu}_2}{s_2}; -\cos \theta \right). \end{aligned}$$

B.3 E_4

$$E_4 = \mathbb{E} \left[\Theta(-Z_1 - \tilde{\mu}_1/s_1) \Theta(-Z_2 - \tilde{\mu}_2/s_2) \right. \\ \left. (e^{s_1 Z_1 + s_2 Z_2 + \tilde{\mu}_1 + \tilde{\mu}_2} - e^{s_1 Z_1 + \tilde{\mu}_1} - e^{s_2 Z_2 + \tilde{\mu}_2} + 1) \right].$$

Each of the four terms may be understood as scales of special cases of the function

$$e_4(a, b) = \mathbb{E} \left[\Theta(-Z_1 - \tilde{\mu}_1/s_1) \Theta(-Z_2 - \tilde{\mu}_2/s_2) e^{a Z_1 + b Z_2} \right]$$

for $a, b \in \mathbb{R}$. Completing the square, $e_4(a, b)$ is given

by

$$\begin{aligned}
& \int_{-\infty}^{-\tilde{\mu}_2/s_2} \int_{-\infty}^{-\tilde{\mu}_1/s_1} \frac{1}{2\pi \sin \theta} \\
& \exp \left(-\frac{1}{2}(\mathbf{z}^\top \Sigma^{-1} \mathbf{z} - 2az_1 - 2bz_2) \right) dz_1 dz_2 \\
& = \int_{\tilde{\mu}_2/s_2}^{\infty} \int_{\tilde{\mu}_1/s_1}^{\infty} \frac{1}{2\pi \sin \theta} \\
& \exp \left(-\frac{1}{2}(\mathbf{z}^\top \Sigma^{-1} \mathbf{z} + 2az_1 + 2bz_2) \right) dz_1 dz_2 \\
& = \frac{\exp \left(\frac{1}{2}(a, b) \Sigma(a, b)^\top \right)}{2\pi \sin \theta} \int_{\tilde{\mu}_2/s_2}^{\infty} \int_{\tilde{\mu}_1/s_1}^{\infty} dz_1 dz_2 \\
& \exp \left(-\frac{1}{2}(\mathbf{z} + \Sigma(a, b)^\top)^\top \Sigma^{-1} (\mathbf{z} + \Sigma(a, b)^\top) \right) \\
& = \Phi((\tilde{\mu}_1/s_1, \tilde{\mu}_2/s_2)^\top - \Sigma(a, b)^\top; \cos \theta) \\
& \exp \left(\frac{1}{2}(a, b) \Sigma(a, b)^\top \right).
\end{aligned}$$

C Stein's lemma for tempered distributions

Lemma 8 (Stein's lemma, tempered distribution). *Let g be a tempered distribution. Then $\mathbb{E}|g(x)| < \infty$ and $\mathbb{E}|g'(x)| < \infty$, where g' is the distributional derivative of g . Furthermore,*

$$\mathbb{E}[Xg(X)] = \mathbb{E}[g'(X)].$$

Proof. This follows from the definition of the derivative for tempered distributions, and the fact that the Gaussian PDF is an element of the Schwartz space. \square

Lemma 9 (Multivariate Stein's lemma, tempered distribution). *Let h be a tempered distribution. Then $\mathbb{E}|h(\mathbf{X})| < \infty$ and $\mathbb{E}|\partial/\partial X_1 h(\mathbf{X})| < \infty$, where $\partial/\partial X_1 h(\mathbf{X})$ is the distributional derivative of h with respect to the first coordinate. Furthermore,*

$$\mathbb{E}[X_1 h(\mathbf{X})] = \sum_{i=1}^n \mathbb{E}[X_1 X_i] \mathbb{E} \left[\frac{\partial}{\partial X_i} h(\mathbf{X}) \right].$$

Proof. First, we prove the statement when X_1, \dots, X_n are independent with standard deviations 1. Stein's lemma says

$$\mathbb{E}[X_1 g(X_1)] = \mathbb{E}[g'(X_1)],$$

for all tempered distributions g . Now for all i and any tempered distribution f ,

$$\begin{aligned}
\mathbb{E}[X_i f(X_1, \dots, X_n)] &= \mathbb{E} \left[\mathbb{E}[X_i f(X_1, \dots, X_n) \mid X_2, \dots, X_n] \right] \\
&= \mathbb{E} \left[(\partial/\partial X_i) f(X_1, \dots, X_n) \right],
\end{aligned}$$

or in vector notation,

$$\text{Cov}[\mathbf{X}, f(\mathbf{X})] = \mathbb{E}[\nabla f(\mathbf{X})].$$

We apply an affine transformation to \mathbf{X} , $\mathbf{Z} = \Sigma^{(1/2)} \mathbf{X} + \boldsymbol{\mu}$. We absorb the affine transform into f , $f(\mathbf{X}) = h(\Sigma^{(1/2)} \mathbf{X} + \boldsymbol{\mu})$ for some h . We have

$$\begin{aligned}
\text{Cov}[\mathbf{Z}, h(\mathbf{Z})] &= \text{Cov}[\Sigma^{(1/2)} \mathbf{X} + \boldsymbol{\mu}, f(\mathbf{X})] \\
&= \text{Cov}[\Sigma^{(1/2)} \mathbf{X}, f(\mathbf{X})] \\
&= \Sigma^{(1/2)} \text{Cov}[\mathbf{X}, f(\mathbf{X})] \\
&= \Sigma^{(1/2)} \mathbb{E}[\nabla f(\mathbf{X})] \\
&= \Sigma \mathbb{E}[\nabla h(\mathbf{Z})].
\end{aligned}$$

We may extract the first entry of the vector, yielding

$$\text{Cov}[Z_1 h(\mathbf{Z})] = \sum_{i=1}^n \mathbb{E}[Z_i Z_1] \mathbb{E}[(\partial/\partial Z_i) h(\mathbf{Z})].$$

\square

D Kernel is infinitely differentiable

Lemma 10. *In the same setting as Theorem 6, the kernel is infinitely differentiable in ρ , s_1 and s_2 .*

Proof. Let $\hat{\phi}_{\rho, s_1, s_2}$ denote the PDF of the bivariate Gaussian having variances s_1^2 and s_2^2 and correlation ρ . Define

$$\kappa(\rho) = \int_{\mathbb{R}^2} \hat{\phi}_{\rho, s_1, s_2}(\mathbf{z}) \psi(z_1) \psi(z_2) dz.$$

The mean value theorem says that for any $a, b \in (-1, 1)$ and $a \leq \rho_1, \rho_2 \leq b$ we have

$$\begin{aligned}
& \kappa(\rho_1) - \kappa(\rho_2) \\
&= \int_{\mathbb{R}^2} (\hat{\phi}_{\rho_1, s_1, s_2}(\mathbf{z}) - \hat{\phi}_{\rho_2, s_1, s_2}(\mathbf{z})) \psi(z_1) \psi(z_2) dz \\
&= (\rho_1 - \rho_2) \int_{\mathbb{R}^2} \frac{\partial \hat{\phi}_{\rho, s_1, s_2}(\mathbf{z})}{\partial \rho} \Big|_{\rho=\rho_3} \psi(z_1) \psi(z_2) dz
\end{aligned}$$

for some $\rho_3 \in (\rho_1, \rho_2)$. So $|\kappa(\rho_1) - \kappa(\rho_2)| \leq M_{a,b} |\rho_1 - \rho_2|$ where $M_{a,b} = \sup_{\rho \in (a,b)} \left| \int_{\mathbb{R}^2} \frac{\partial \hat{\phi}_{\rho, s_1, s_2}(\mathbf{z})}{\partial \rho} \Big|_{\rho=\rho_3} \psi(z_1) \psi(z_2) dz \right|$.

Note that $M_{a,b}$ is finite because each element in the supremum is the integral of a Schwartz function. The same argument applies to derivatives of any order of, since each derivative is also an element of the Schwartz space.

The same argument applies to s_1 and s_2 . \square

E Derivative at endpoints

Lemma 11. *In the same setting as Theorem 6, with the additional assumptions that ψ is continuous almost everywhere, the expression for λ_3 extend to $\rho \in [-1, 1]$ provided the expression for λ_3 is finite over $[-1, 1]$.*

Proof. Note that κ is continuous in ρ since

$$\begin{aligned} & \lim_{\rho \rightarrow c} \int_{\mathbb{R}^2} \phi(\mathbf{z}) \psi(s_1 z_1) \psi(s_2(z_1 \rho + z_2 \sqrt{1 - \rho^2})) d\mathbf{z} \\ &= \int_{\mathbb{R}^2} \phi(\mathbf{z}) \psi(s_1 z_1) \lim_{\rho \rightarrow c} \psi(s_2(z_1 \rho + z_2 \sqrt{1 - \rho^2})) d\mathbf{z}, \end{aligned}$$

with the interchange of the limit being justified by dominated convergence, since

$$\begin{aligned} & \phi(\mathbf{z}) \psi(s_1 z_1) \psi(s_2(z_1 \rho + z_2 \sqrt{1 - \rho^2})) \\ & \leq \phi(\mathbf{z}) \max\{\psi^2(s_1 z_1), \psi^2(s_2(z_1 \rho + z_2 \sqrt{1 - \rho^2}))\} \\ & \leq \phi(\mathbf{z}) (\psi^2(s_1 z_1) + \psi^2(s_2(z_1 \rho + z_2 \sqrt{1 - \rho^2}))), \end{aligned}$$

which has integral $\mathbb{E}[\psi^2(s_1 Z_1)] + \mathbb{E}[\psi^2(s_2 Z_1)]$.

Then supposing WLOG $\rho_0 < \rho_1$ for $\rho_0, \rho_1 \in [-1, 1]$,

$$\begin{aligned} |\kappa(\rho_1) - \kappa(\rho_0)| &= \lim_{a \rightarrow \rho_0^+} \lim_{b \rightarrow \rho_1^-} |\kappa(b) - \kappa(a)| \\ &\leq \lim_{a \rightarrow \rho_0^+} \lim_{b \rightarrow \rho_1^-} M_{-1,1} |b - a| \\ &= M_{-1,1} |\rho_1 - \rho_0|, \end{aligned}$$

where κ and $M_{-1,1}$ are as in Appendix D. Note $M_{-1,1}$ is finite since

$$\begin{aligned} M_{-1,1} &= \sup_{\rho \in (-1,1)} \left| \frac{\partial}{\partial \rho} \int_{\mathbb{R}^2} \hat{\phi}_{1,1,1}(\mathbf{z}) \psi(s_1 z_1) \right. \\ &\quad \left. \psi(s_2(z_1 \rho + z_2 \sqrt{1 - \rho^2} z_2)) d\mathbf{z} \right| \\ &= \sup_{\rho \in (-1,1)} \left| \int_{\mathbb{R}^2} \phi(\mathbf{z}) \psi(s_1 z_1) \psi'(s_2(z_1 \rho + z_2 \sqrt{1 - \rho^2})) \right. \\ &\quad \left. s_2 \left(z_1 + \frac{z_2 \rho}{(1 - \rho^2)^{1/2}} \right) d\mathbf{z} \right| \\ &= \sup_{\rho \in (-1,1)} \left| s_1 s_2 \mathbb{E}[\psi'(s_1 Z_1) \psi'(s_2 Z_2)] \right| < \infty, \end{aligned}$$

where the last equality is due to two applications of Stein's lemma, as in the proof of Theorem 6.

κ therefore has finite derivative on $[-1, 1]$. We have

$$\begin{aligned} \frac{d\kappa}{d\rho} &= \int_{\mathbb{R}^2} \phi(\mathbf{z}) \psi(s_1 z_1) \psi'(s_2(z_1 \rho + z_2 \sqrt{1 - \rho^2})) \\ &\quad s_2 \left(z_1 + \frac{z_2 \rho}{(1 - \rho^2)^{1/2}} \right) d\mathbf{z}. \end{aligned}$$

Two applications of Stein's lemma as in the proof of Theorem 6 gives the desired result. \square

F Example eigenvalues

F.1 GELU

We would like to evaluate

$$\begin{aligned} & \sigma^2 \mathbb{E}[(\Phi(\sigma \|\mathbf{x}\| Z_1) + (\sigma \|\mathbf{x}\| Z_1) \phi(\sigma \|\mathbf{x}\| Z_1)) \\ & \quad (\Phi(\sigma \|\mathbf{x}\| Z_2) + (\sigma \|\mathbf{x}\| Z_2) \phi(\sigma \|\mathbf{x}\| Z_2))]. \end{aligned}$$

Expanding, the first term may be related to the result of Williams (1997) since

$$\begin{aligned} & \mathbb{E}[\Phi(\sigma \|\mathbf{x}\| Z_1) \Phi(\sigma \|\mathbf{x}\| Z_2)] \\ &= \frac{1}{4} \mathbb{E}[(1 + \text{erf}(\sigma \|\mathbf{x}\| Z_1 / \sqrt{2})) (1 + \text{erf}(\sigma \|\mathbf{x}\| Z_2 / \sqrt{2}))] \\ &= \frac{1}{4} \left(1 + \mathbb{E}[\text{erf}(\sigma \|\mathbf{x}\| Z_1 / \sqrt{2}) \text{erf}(\sigma \|\mathbf{x}\| Z_2 / \sqrt{2})] \right) \\ &= \frac{1}{4} \left(1 + \frac{2}{\pi} \sin^{-1} \frac{\sigma^2 \|\mathbf{x}\|^2 \cos \theta}{1 + \sigma^2 \|\mathbf{x}\|^2} \right). \end{aligned}$$

The middle cross-terms are equal by exchangeability of Z_1 and Z_2 , and are given by

$$h(\beta) = \mathbb{E}[\Phi(\beta \sigma \|\mathbf{x}\| Z_1) (\sigma \|\mathbf{x}\| Z_2) \phi(\sigma \|\mathbf{x}\| Z_2)]$$

evaluated at $\beta = 1$. Differentiating under the integral, we obtain the initial value problem

$$\begin{aligned} \frac{dh}{d\beta} &= \frac{\sigma^2 \|\mathbf{x}\|^2 \cos \theta}{2\pi} \\ &\quad (1 + \sigma^2 \|\mathbf{x}\|^2 (1 + \beta^2 + \sigma^2 \|\mathbf{x}\|^2 \beta^2 \sin^2 \theta))^{-3/2}, \\ h(0) &= 0, \end{aligned}$$

with solution $h(\beta)$

$$\frac{\cos \theta \sigma^2 \|\mathbf{x}\|^2 \beta}{2\pi (\sigma^2 \|\mathbf{x}\|^2 + 1) \sqrt{\beta^2 \sigma^4 \|\mathbf{x}\|^4 \sin^2 \theta + (\beta^2 + 1) \sigma^2 \|\mathbf{x}\|^2 + 1}}. \quad (9)$$

The last term simply involves collecting the arguments of the exponentials inside the integral.

$$\begin{aligned} & \sigma^2 \|\mathbf{x}\|^2 \mathbb{E}[Z_1 Z_2 \phi(\sigma \|\mathbf{x}\| Z_2) \phi(\sigma \|\mathbf{x}\| Z_1)] \\ &= \frac{\sigma^2 \|\mathbf{x}\|^2}{2\pi} \frac{\cos \theta}{(1 + 2\sigma^2 \|\mathbf{x}\|^2 + \sigma^4 \|\mathbf{x}\|^4 \sin^2 \theta)^{3/2}}. \end{aligned}$$

F.2 ELU

The generalised derivative of the ELU is

$$\phi'(z) = \Theta(z) + \delta(z)z + \Theta(-z)e^z + \delta(-z)(1 - e^z).$$

The second and last terms may be treated as zero since they vanish under integration. We would like to evaluate

$$\begin{aligned} \sigma^2 \mathbb{E}[(\Theta(\sigma\|\mathbf{x}\|Z_1) + \Theta(-\sigma\|\mathbf{x}\|Z_1)e^{\sigma\|\mathbf{x}\|Z_1}) \\ (\Theta(\sigma\|\mathbf{x}\|Z_2) + \Theta(-\sigma\|\mathbf{x}\|Z_2)e^{\sigma\|\mathbf{x}\|Z_2})]. \end{aligned}$$

Expanding, the first term is given by Sheppard's identity.

The cross-terms are equal by exchangeability of Z_1 and Z_2 , and can be evaluated by completing the square of the exponential terms.

$$\begin{aligned} & \mathbb{E}[\Theta(\sigma\|\mathbf{x}\|Z_1)\Theta(-\sigma\|\mathbf{x}\|Z_2)e^{\sigma\|\mathbf{x}\|Z_2}] \\ &= \mathbb{E}[\Theta(Z_1 + \sigma\|\mathbf{x}\| \cos \theta)\Theta(-Z_2 - \sigma\|\mathbf{x}\|)]e^{\frac{1}{2}\sigma^2\|\mathbf{x}\|^2} \\ &= e^{\frac{1}{2}\sigma^2\|\mathbf{x}\|^2}\Phi(\sigma\|\mathbf{x}\| \cos \theta, -\sigma\|\mathbf{x}\|; -\cos \theta). \end{aligned}$$

The last term is evaluated similarly,

$$\begin{aligned} & \mathbb{E}[\Theta(-\sigma\|\mathbf{x}\|Z_1)\Theta(-\sigma\|\mathbf{x}\|Z_2)e^{\sigma\|\mathbf{x}\|(Z_1+Z_2)}] \\ &= e^{\sigma^2\|\mathbf{x}\|^2(1+\cos \theta)}\mathbb{E}[\Theta(-Z_1 - \sigma\|\mathbf{x}\|(1+\cos \theta)) \\ & \quad \Theta(-Z_2 - \sigma\|\mathbf{x}\|(1+\cos \theta))] \\ &= e^{\sigma^2\|\mathbf{x}\|^2(1+\cos \theta)} \\ & \quad \Phi(-\sigma\|\mathbf{x}\|(1+\cos \theta), -\sigma\|\mathbf{x}\|(1+\cos \theta); \cos \theta). \end{aligned}$$

G Experimental details

G.1 Shallow models

We largely followed the experimental protocol originally established in (Hernández-Lobato and Adams, 2015) which was designed to assess uncertainty estimates of Bayesian neural networks. Since we used GPs, we found it necessary to deviate in several places as follows.

We performed GP regression analytically, and hence couldn't scale up to the larger datasets. We excluded Song Year and uniformly subsampled the Protein dataset down to 10,000 datapoints.

We had four hyperparameters to tune; first layer weight variance, first layer bias variance, final layer weight variance, data noise variance. We excluded the final bias to reduce the search space. We allowed these to vary in the below ranges.

$$\begin{aligned} \sigma_{w0}^2 & \in \{10, 3.5, 3, 2.5, 2, 1.5, 1, 0.5, 0.1\} \\ \sigma_{b0}^2 & \in \{10, 3.5, 3, 2.5, 2, 1.5, 1, 0.5, 0.1\} \\ \sigma_{w1}^2 & \in \{10, 3.5, 3, 2.5, 2, 1.5, 1, 0.5, 0.1\} \\ \sigma_{\epsilon}^2 & \in \{1e0, 1e-1, 1e-2, 1e-3, 1e-4, 1e-5\} \end{aligned}$$

To choose hyperparameters, we ran a full grid search over these values using 70% for training and 20% as a validation set. We selected according to NLL on the validation set (setting according to marginal likelihood

produced comparable though slightly worse results). Unlike the original protocol, we performed this tuning only on the first train/test split of each dataset, holding hyperparameters constant for the remaining splits. The leaky ReLU kernel has an additional parameter, α , corresponding to the negative slope. This was fixed at $\alpha = 0.2$.

Test/train splits were randomly shuffled but used the same random seed across kernels. Experiments were repeated 20 times for all datasets except Protein which only repeated 5 times.

Following previous works reporting on the benchmark, we include results in tabular format in table 2. These are consistent with figure 6.

G.2 Deep models

We provide RMSE plots for each dataset in Figure G.2.

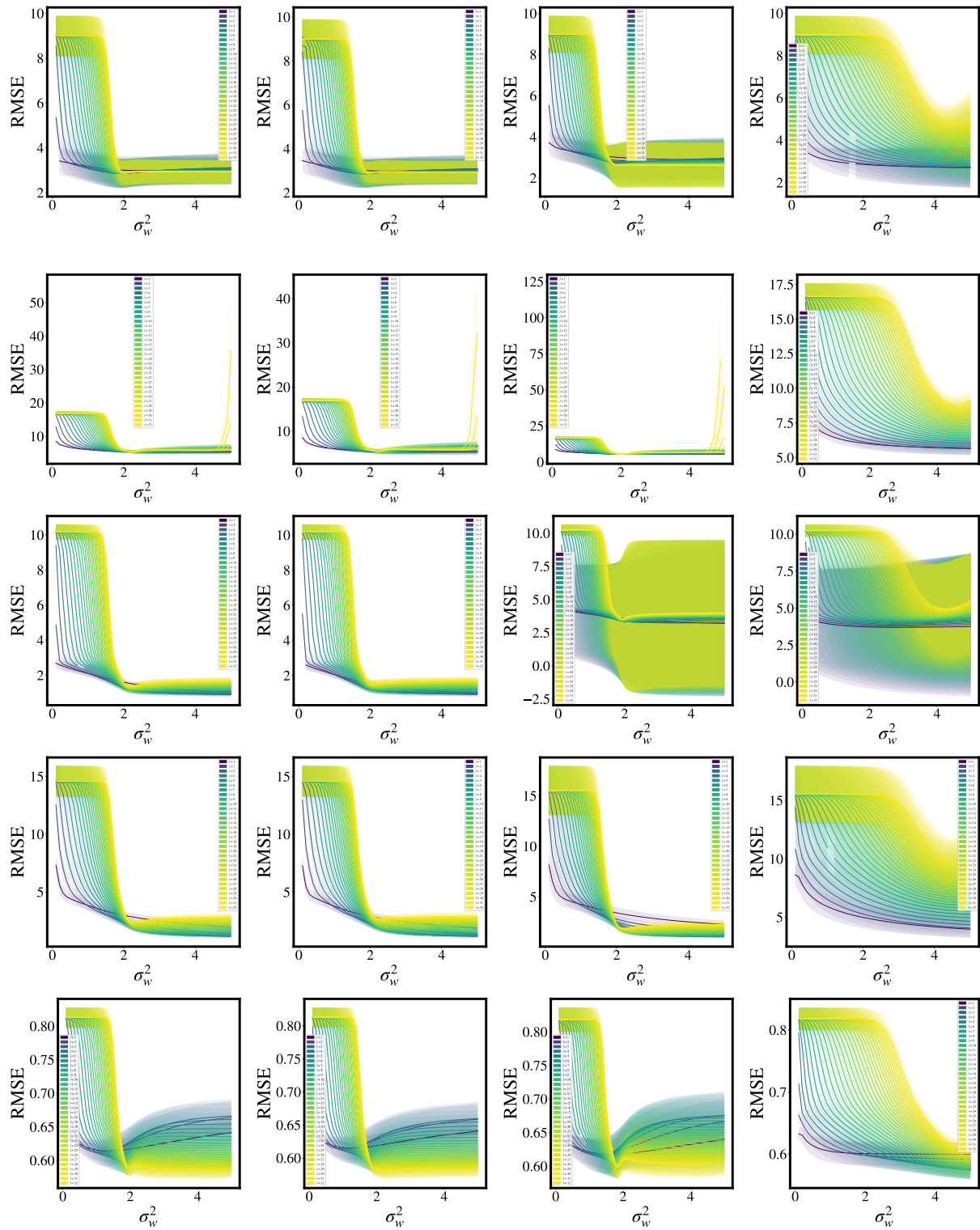


Figure 9: RMSE as depth and σ_w^2 varies. (Top - Bottom) Boston, Concrete, Energy, Yacht, Wine.

Table 2: Performance on benchmark regression datasets. Mean ± 1 standard error.

	NLL				RMSE			
	GELU	ReLU	L. ReLU	ERF	GELU	ReLU	L. ReLU	ERF
Boston	2.54 \pm 0.05	2.54 \pm 0.05	2.55 \pm 0.05	2.48 \pm 0.05	3.09 \pm 0.18	3.11 \pm 0.18	3.14 \pm 0.18	2.89 \pm 0.16
Concrete	3.05 \pm 0.01	3.05 \pm 0.01	3.05 \pm 0.01	3.07 \pm 0.01	5.09 \pm 0.12	5.04 \pm 0.12	4.99 \pm 0.12	5.08 \pm 0.12
Energy	0.82 \pm 0.02	0.83 \pm 0.02	0.86 \pm 0.02	0.88 \pm 0.03	0.59 \pm 0.02	0.57 \pm 0.02	0.58 \pm 0.02	0.64 \pm 0.02
Kin8nm	-1.18 \pm 0.01	-1.19 \pm 0.01	-1.20 \pm 0.01	-1.18 \pm 0.01	0.07 \pm 0.00	0.07 \pm 0.00	0.07 \pm 0.00	0.07 \pm 0.00
Naval	-7.89 \pm 0.00	-7.87 \pm 0.00	-7.87 \pm 0.00	-7.88 \pm 0.00	0.00 \pm 0.00	0.00 \pm 0.00	0.00 \pm 0.00	0.00 \pm 0.00
Power	2.88 \pm 0.01	2.97 \pm 0.03	2.88 \pm 0.01	2.88 \pm 0.01	3.93 \pm 0.04	3.65 \pm 0.04	3.89 \pm 0.04	3.91 \pm 0.04
Protein	2.94 \pm 0.01	2.94 \pm 0.01	2.99 \pm 0.00	2.82 \pm 0.01	4.01 \pm 0.02	3.99 \pm 0.02	4.22 \pm 0.02	3.92 \pm 0.02
Wine	-0.04 \pm 0.04	0.01 \pm 0.04	-0.06 \pm 0.04	-0.13 \pm 0.04	0.65 \pm 0.01	0.66 \pm 0.01	0.66 \pm 0.01	0.60 \pm 0.01
Yacht	0.02 \pm 0.07	0.48 \pm 0.09	0.52 \pm 0.09	0.17 \pm 0.07	0.37 \pm 0.04	0.59 \pm 0.08	0.60 \pm 0.08	0.51 \pm 0.06